Primljen / Received: 22.9.2024.
Ispravljen / Corrected: 21.6.2025.
Prihvaćen / Accepted: 15.7.2025.
Dostupno online / Available online: 10.10.2025.

Seismic modification factors for box girder bridges using a proposed pushover technique incorporating torsional vibration modes

Authors:



Soumia Aouiss, MSc. CE s.aouissi@univ-djelfa.dz



Assist.Prof. Mouloud Ouanani, PhD. CE m.ouanani@univ-djelfa.dz
Corresponding author



Assist.Prof. Khaled Sandjak, PhD. CE k.sandjak@univ-boumerdes.dz



Assist.Prof. Amar Louzai, PhD. CE Amar.louzai@yahoo.fr

Ziane Achour University, Algeria
Department of Civil Engineering
Laboratory for Seismic Engineering and
Structural Dynamics (LGSDS)

Soumia Aouiss, Mouloud Ouanani, Khaled Sandjak, Amar Louzai

Research Paper

Seismic modification factors for box girder bridges using a proposed pushover technique incorporating torsional vibration modes

This paper presents the results of numerical investigations on seismic modification factors (R) for algerian box girder bridges (BGBs) with both equal and unequal pier heights, using a proposed pushover technique that incorporates torsional vibration modes. In the first part, the BGB referenced in a project by the Algerian Highway National Agency is selected to evaluate the components of the R-factor in the transverse direction. Conventional pushover analysis (CPA), employing the elastic first mode, uniform, and upper-bound lateral load patterns, as well as the proposed pushover technique, is conducted. The results of CPA and the proposed pushover technique for the reference BGB are examined in terms of R-factor components, including overstrength (Ω) and global ductility (R- μ), and are compared with those obtained using the incremental dynamic analysis (IDA) technique. The findings indicate strong agreement between the proposed pushover technique and the IDA technique.

Key words:

box girder bridges (BGBs), torsional vibration modes, the proposed pushover and IDA techniques, R-factor, over-strength (Ω) , global ductility $(R-\mu)$

Prethodno priopćenje

Soumia Aouiss, Mouloud Ouanani, Khaled Sandjak, Amar Louzai

Faktori modifikacije seizmičkog odziva za sandučaste gredne mostove primjenom metode postupnog guranja koja uključuje torzijske oblike titranja

U ovom su radu predstavljeni rezultati numeričkih istraživanja faktora modifikacije seizmičkog odziva (R) za alžirske sandučaste gredne mostove sa stupovima jednakih i nejednakih visina primjenom predložene metode postupnog guranja, koja uključuje torzijske oblike tiranja. U prvom je dijelu odabran SGM u sklopu projekta Alžirske nacionalne agencije za autoceste radi procjene komponenti R-faktora u poprečnome smjeru. Provedena je konvencionalna metoda postupnog guranja (CPA), pri čemu je primijenjena modalna raspodjela bočnih opterećenja uporabom prvog vlastitog oblika elastičnog sustava, jednolika raspodjela bočnih opterećenja i gornja granična raspodjela bočnih opterećenja, kao i predložena metoda postupnog guranja. Rezultati CPA-e i predložene metode postupnog guranja za referentni SGM ispitani su u odnosu na komponente R-faktora, uključujući povećanu nosivost (Ω) i globalnu duktilnost (R- μ), te su uspoređeni s rezultatima dobivenima primjenom inkrementalne dinamičke analize (IDA). Rezultati upućuju na znatno podudaranje između predložene metode postupnog guranja i inkrementalne dinamičke analize.

Kliučne riječi:

sandučasti gredni mostovi (SGM), torzijske vibracije, predložene metode postupnog guranja i inkrementalne dinamičke analize (IDA), R-faktor, povećana čvrstoća (Ω), globalna duktilnost (R-μ)

1. Introduction

Long box girder bridges (BGBs) are vital elements of national transportation networks, and their serviceability during major earthquake ground motions is crucial for passenger safety. In Algeria, where the demand for transport infrastructure is high [1, 2], BGBs have undergone rapid development owing to their aesthetic appeal and cost-effectiveness. This growth has been driven by several factors, including expertise in the cantilever construction method, the need to span longer distances, the efficiency of construction techniques, and ease of maintenance. A key element in the seismic design of bridges is the response modification factor (R factor), which is used to estimate the design earthquake forces on bridge structures. This factor reflects a structure's capacity to undergo inelastic deformations while maintaining its load-bearing ability. By dissipating energy, seismic forces considered during design are reduced, thereby improving earthquake resistance and lowering construction costs. In bridge structures, the R factor depends on the seismic resistance system. For example, in continuous box girder bridges, structural continuity and high torsional rigidity enhance energy dissipation, resulting in higher R values. In contrast, simply supported girder bridges exhibit lower ductility and overstrength, leading to lower R factors. Base-isolated bridges, which use isolation devices to improve energy dissipation, achieve significantly higher R values.

The R factor, defined as the ratio of the force that a bridge would develop if it responded elastically to the design seismic action to the design base shear, represents an essential design parameter. This factor is denoted as (q) in the European Code EC8 [3] and referred to as the response modification factor (R) in the American Code UBC [4] and the Algerian Bridge Seismic Design Code [5]. Assessing this parameter is important in the seismic design of BGBs, as well as in the verification and calibration of seismic design codes. Evaluating this factor is therefore crucial not only for ensuring the safety and reliability of this class of bridges in practice but also for refining engineering standards and advancing the development of more effective seismic design regulations.

The analytical estimation of the R factor is typically based on nonlinear static pushover analysis (NLSPA) of the global bridge structure. This method is widely used to evaluate the seismic behaviour of bridges [6-8], providing a more cost-effective computational approach than incremental dynamic analysis (IDA), which demands substantial computational resources and a representative set of earthquake records for high-intensity events [9-11].

Numerous researchers have evaluated the components of the R factor for bridge structures, such as the overstrength factor and global ductility, using NLSPA methods [12-14]. For instance, Sai et al. [13] investigated the R factor under different seismic zonal conditions for bridges with unequal pier heights and found that both ductility and overstrength decrease as the seismic zone factor increases.

In addition, Muhammad et al. [14] determined the R factor of three bridges using NLSPA and reported values ranging from 4.5 to 5 in both the longitudinal and transverse directions. Michael et al. [15] investigated the seismic response of isolated bridges and concluded that, compared with the values specified in the AASHTO code, the R factor is lower for non-isolated bridges. However, several studies [16-17] have shown that the contribution of higher modes can be used to quantify the R factor of bridge structures. For instance, Ehsan and Shooshtari [16] proposed a new adaptive pushover technique to account for higher-mode effects in accurately estimating the seismic response of bridges. They recommended the method for application in seismic performance evaluation of bridges for engineering purposes. Alessandro et al. [17] introduced an incremental modal pushover analysis for both regular and irregular bridges, incorporating higher modes through multimodal (MPA) and uniform (UPA) load patterns, together with IDA. They found that MPA produces a capacity curve closely matching that obtained from IDA. The NLSPA technique must therefore be specifically adapted for both regular and irregular bridges to account for higher vibration modes, particularly torsional modes, enabling a more accurate determination of the R factor and the overall dynamic behaviour of bridges.

As highlighted in previous studies, torsional vibration modes are generally excluded from inelastic pushover analyses used to estimate the R factor for bridges. This issue is particularly critical for BGBs with unequal pier heights, where the contribution of torsional modes is significant. Moreover, seismic design codes lack specific provisions addressing the R factor for this class of bridges. This gap creates uncertainty in both design and evaluation, as engineers lack a standardised approach for incorporating the R factor into their calculations. The absence of such guidelines may result in inconsistent practices and potentially compromise the safety and reliability of these structures.

In the first part of this paper, the main results of the numerical investigation of the R factor components, including the overstrength factor and global ductility, for the reference BGB are presented. This investigation employs NLSPA, comprising conventional pushover analysis (CPA) and the proposed pushover techniques. The results from these techniques are compared with those obtained using the inelastic IDA method, based on a suite of eight historical earthquake records with ground motion intensities ranging from 0.22g to 0.60g.

In the second part, eighteen continuous prestressed BGBs, with both equal and unequal pier heights representing regular and irregular configurations, are analysed to estimate the R factor in the transverse direction using the proposed pushover technique. The resulting R factor values are then compared with those recommended by the Algerian Highway Bridge Design Seismic Regulation (RPOA). Recommendations for revising this factor for BGBs will be submitted to the Algerian Ministry of Public Works for further consideration and potential implementation.

2. Description of the reference BGB

The reference box girder bridge, selected from a project developed by the Algerian National Highway Agency, is used to estimate the components of the response modification factor (R factor) for highway box girder bridges (BGBs) under NLSPA, including CPA, the proposed pushover techniques, and the IDA method. The continuous BGB under study connects two major economic cities, Tizi-Ouzou and Bejaia, in northern Algeria.

The bridge has a total length of 248.80 m and comprises four continuous box girders, with two mid-spans of 81.80 m and two end spans of 42.60 m, as shown in Figure 1.a. Classified as strategic (importance category 1), it is located on a firm site (S2) with a peak ground acceleration (PGA) of 0.33g in accordance with the highway bridges design seismic regulations [5]. The deck is straight in plan, with a total width of 13.80 m and a constant depth of 3.32 m (Figure 1.b). The moments of inertia of the deck cross-section about the two in-plane axes, as well as the torsional moment of inertia about the longitudinal axis, are given in Figure 1.b.

The longitudinally prestressed concrete (PC) deck is supported by two reinforced concrete (RC) piers of unequal height, 15.95 m and 26.65 m, together with a central pier 50.35 m high. The deck is also supported by elastomeric bearings on each of the two seat-type pile abutments.

The piers have identical hollow cross-sections measuring 5.00 \times 7.50 m with a wall thickness of 0.30 m (Figure 1.c). They are founded on concrete pile foundations and monolithically connected to the deck. Owing to the rigidity of the foundation system, soil-structure interaction (SSI) is not considered in this study.

3. Modelling of the reference BGB

A nonlinear analytical model with lumped masses and frame elements for the reference BGB, shown in Figure 1, was developed using the general-purpose structural analysis software CSI Bridge [18]. The bridge deck was modelled with elastic beam elements, as it was expected to remain elastic during seismic loading, while the piers were represented by nonlinear frame elements with material properties corresponding to cracked reinforced concrete. The piers, which constituted the most critical components of this type of bridge, were modelled with an elastic region and two plastic hinge regions concentrated at the top and bottom. The plastic hinge regions were defined by moment-rotation curves based on the Caltrans model [19]. The plastic hinge length (L_p) was calculated using the formulas provided in [20].

$$L_p = 0.08 \cdot L + 0.022 \cdot f_v \cdot d_{bl} \ge 0.044 \cdot f_v \cdot d_{bl} \text{ [mm, MPa]}$$
 (1)

where L represents the length of the piers, while f_{γ} and d_{bl} denote the yield strength and the diameter of the longitudinal reinforcement bars, respectively.

The compressive strengths of the concrete used in this study for seismic design were 30 MPa for the RC piers and 35 MPa for the PC bridge deck at 28 days. The design parameters of the longitudinal reinforcing bars (Ø25) were: yield strength $f_v = 500$ MPa, elastic modulus $E_s = 200000$ MPa and ultimate strength $F_u = 550$ MPa. The transverse reinforcement (stirrups) was assumed to consist of 16 mm diameter bars (Ø16) spaced at 100 mm in both piers. Gravity loads, comprising dead loads and 20 % of live loads [3, 5], were included in the analysis.

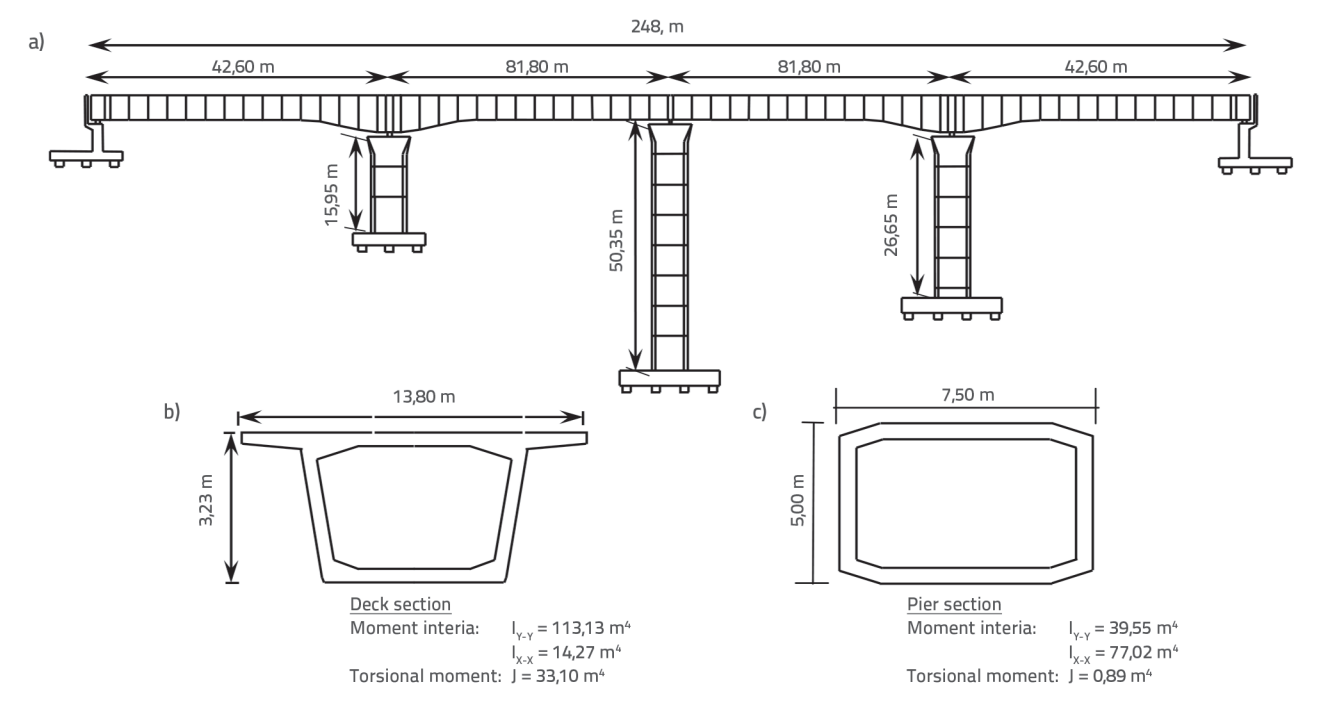


Figure 1. Description of the reference BGB: a) Schematic elevation view of the reference BGB; b) Typical cross-section of the BGB deck; c) Typical cross-section of the BGB piers

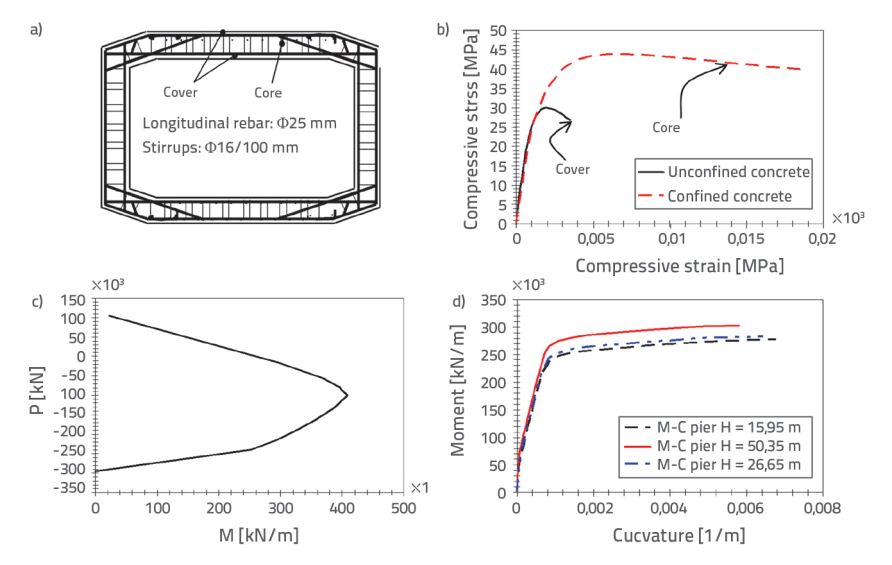


Figure 2. Pier section analysis results: a) Pier cross-section geometry; b) Stress-strain relationship of unconfined and confined concrete; c) Axial force-bending moment (P-M) interaction diagram, (d) Moment-curvature (M-C) diagram

The nonlinearity of reinforced concrete (R.C.) piers was represented by plastic hinges at the ends of the bridge piers, with consideration of the P- Δ effect. The associated steel reinforcing sections were divided into two zones:

- the cover concrete region and
- the core concrete region (Figure 2.a).

The Mander concrete model [21] was adopted for the bridge pier section analysis (Figure 2.b). Both ends of the bridge piers were modelled with flexural (P-M) hinges in the plastic regions to represent the nonlinear seismic response of R.C. bridges under severe seismic excitations (Figure 2.c).

According to EC8[3], the dominant mode of failure in earthquakeresistant structures is bending, which ensures ductile behaviour and improved seismic performance, unlike shear or buckling failure, which is typically more abrupt and difficult to control. However, the shear failure mode can significantly affect the overall seismic response of squat bridge piers. These piers are particularly vulnerable to shear failure at the base, where shear stress may exceed the material's shear capacity. The shear capacity of a squat pier generally depends on its cross-sectional geometry, the compressive strength of the concrete, and the amount of reinforcing steel provided.

In conclusion, although squat piers are usually designed to fail in flexure, the role of shear behaviour should not be neglected. The design must ensure that the shear capacity is sufficient to withstand seismic excitations. Adequate transverse reinforcement and a detailed analysis of shear stress distribution are essential to prevent shear failure under seismic loading.

A general-purpose structural analysis code, CSI Bridge [18], was employed to simulate the stress-strain behaviour of unconfined and confined concrete, as well as the P-M interaction and

moment-curvature (M-C) diagrams (Figure 2(d)). The results of the pier section analysis are presented in Figure 2

The bridge deck is restrained in the lateral and vertical directions at both rigid seat-type pile abutments, while its longitudinal movement is governed by the flexibility of high-damping rubber bearing (HDRB) devices installed on each abutment. The mechanical properties of the HDRB devices initial stiffness. yield strength, and post-yield stiffness are determined in accordance with the procedures specified in the design guidelines [22, 23] for nonlinear analysis. The translational masses (mi) along the three global directions of the bridge, corresponding to the X, Y, and Z axes, are assigned to each node of the nonlinear analytical model of the reference BGB.

It should be noted that the torsional vibration modes and the outcomes of the pushover analysis in the lateral direction of the bridge are also influenced by the torsional masses about the longitudinal axis of the bridge, as expressed by the following formula:

$$m_{x,i} = \frac{L_{trib} \cdot d_w^2}{12} \tag{2}$$

where m_{i} represents the translational mass of the bridge deck and column tributary to node (i), L_{trib} is the tributary length assigned to the considered node, and d_{w}^{2} is the square of the bridge deck width.

The nonlinear analytical model of The reference box girder bridge (BGB), including the lateral load pattern for pushover analysis and the monitored control point, was developed using the Finite Element Method (FEM), as illustrated in Figure 3.

A pushover analysis of the bridge was conducted using a displacement-controlled method in which the bridge structure was incrementally displaced until a predefined limit was reached. This approach enables the capture of the nonlinear softening behaviour of the structure by monitoring displacements at reference points, such as the top node of the central pier or the midspan of the superstructure, facilitating the identification of structural changes and potential failure points.

In this study, the mid-span of the bridge deck connected to the central pier was selected as the monitored control point in the pushover analysis. This location was considered critical for determining the seismic modification factor (R) of box girder bridges. Monitoring this point enabled a more accurate assessment of the structural response, allowing identification of the maximum vulnerability zone and tracking of damage progression throughout the analysis.

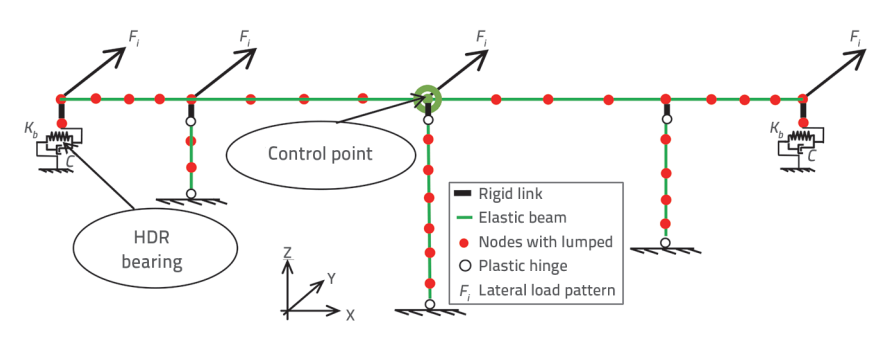


Figure 3. Schematic of the nonlinear analytical model with lateral load pattern for the pushover analysis of the reference box girder bridge (BGB)

4.1.3. Upper-bound lateral load pattern

In this pushover analysis procedure, only the first two vibration modes influence the seismic response of the structure [27]. The distribution vector of lateral loads in the lateral direction of the bridge deck using the Upper-Bound (UB) load pattern $F_{\textit{LUB}}$ is given as follows:

$$F_{i,UB} = \omega_1^2 m_i \Phi_{i1.} + \omega_2^2 m_i \Phi_{i2.} \left(\frac{q_2}{q_1} \right)$$
 (5)

4. Nonlinear static pushover analysis (NLSPA)

4.1. Conventional pushover analysis

The conventional pushover analysis, as presented in references [11, 24], is a static nonlinear procedure in which the magnitude of structural loading is monotonically increased according to a predefined reference load pattern. This method facilitates the identification of the sequential occurrence of limit-state damages, including cracking, plastic hinging, and structural element failure.

In this study, a nonlinear static pushover analysis (NSPA) is performed using three predefined lateral load patterns to estimate the components of the R-factors.

4.1.1. Elastic first mode lateral load pattern

This method assumes that the structural response is governed solely by the first mode, and is applicable when the participating mass ratio exceeds 80 % of the total mass. In this model, the applied lateral forces are proportional to the product of the mass and first-mode shape [25, 26], expressed as

$$F_i = M \cdot \Phi_n^1 \tag{3}$$

where M represents the mass matrix and Φ_n^1 denotes the mode shape of the first mode in the given direction.

4.1.2. Uniform lateral load pattern

This model is based on a uniform distribution of lateral forces proportional to the tributary mass at each point, and is expressed as follows [22]:

$$f_i = m_i = \rho_{RC} \cdot A \cdot L_{trib} \tag{4}$$

where ρ_{RC} designates the density of concrete, A represents the superstructure cross-section area, and L_{trib} is defined previouslyin Eq.(2).

where ω_i and Φ_i (i = 1 i 2) denote respectively the natural frequencies and the corresponding vibration mode shapes for the first and second modes, the term $(\mathbf{q_2/q_1})$ represents the UB of the contribution ratio of the second mode, given by the following expression:

$$\frac{q_2}{q_1} = \frac{\Gamma_2 \cdot D_2}{\Gamma_1 \cdot D_1} \tag{6}$$

where Γ_n (n = 1, 2) and D $_n$ (n = 1, 2) and represent the modal participation factors and the spectral displacements, respectively, derived from the elastic displacement response spectrum.

4.2. Proposed pushover technique

This technique incorporates torsional vibration modes into nonlinear static pushover analysis, which are typically neglected in conventional pushover procedures. It achieves this by combining bridge deck modal forces in the lateral direction (f_{vy}) and torsional moments (M_{vy}) about the longitudinal axis. Based on spectral dynamic analysis [28], the modal lateral force and torsional moment at each node of the nonlinear analytical bridge model for the considered modes are expressed as follows:

$$f_{vij} = \Gamma_{vj} \cdot \Phi_{vil} \cdot m_{vi} \cdot S_{avj} \tag{7}$$

$$M_{\theta ij} = \Gamma_{vi} \cdot \Phi_{\theta ij} \cdot I_{\theta i} \cdot S_{avj} \tag{8}$$

where Γ_{vj} represents the modal participation factor of the j^{th} mode for excitation in the lateral direction (i.e., Y-axis); Φ_{vj} and $\Phi_{\theta vj}$ are the mode shape vectors of the j^{th} mode in the lateral direction and in torsion about the longitudinal direction (i.e., X-axis), respectively; S_{vvj} is the spectral acceleration associated with the j^{th} mode of vibration due to excitation in the lateral direction; and is the torsional mass of the i^{th} bridge deck node. The modal lateral shear (SS_{vj}) in the lateral direction and the total torsional moment $(SM_{\theta vj})$ at each i^{th} node of the bridge superstructure, corresponding to each vibration mode, are determined using Eqs. (9) and (10), respectively.

$$SS_{y_{ij}} = \sum_{k=i}^{N} f_{y_{k_j}} \tag{9}$$

$$SM_{\theta ij} = \sum_{k=i}^{N} M_{\theta_{kj}} \tag{10}$$

fykj and $M_{\theta kj}$ indicate the forces in the lateral direction and the torsional moments of the k^{th} bridge deck node, respectively, associated with each j^{th} mode, and N is the number of bridge deck nodes.

The combined modal shear (CSS_y) at each ith node of the deck in the lateral translational direction, and the combined modal total torsional moment (CSM_0) of the ith node about the longitudinal bridge deck axis, are evaluated using the Square Root of the Sum of the Squares (SRSS) rule using Eqs. (11) and (12), respectively.

$$CSS_{y_i} = \sqrt{\sum_{j=1}^{m} SS_{y_{ij}}^2}$$
 (11)

$$CSM_{\theta_i} = \sqrt{\sum_{j=1}^{m} SM_{\theta_{ij}}^2}$$
 (12)

where m is the number of modes used to estimate the combined responses.

The components of the load pattern vectors at each bridge node in Eqs. (13) and (14) were determined by subtracting the combined modal shear and combined total torsional moment of consecutive nodes of the bridge deck, as shown in the following equations:

$$\begin{cases} F_{y_i} = CSS_{y_i} - CSS_{y_{i+1}} & i < N \\ F_{y_i} = CSS_{y_i} & i = N \end{cases}$$
(13)

$$\begin{cases} M_{\theta_i} = CSM_{\theta_i} - CSM_{\theta_{i+1}} & i < N \\ M_{\theta_i} = CSM_{\theta_i} & i = N \end{cases}$$
(14)

The load pattern components and along the excitation lateral direction (Y-axis) are evaluated using Eqs. (15) and (16), respectively.

$$\overline{F}_{y_i} = F_{y_i} \cdot \frac{\Delta V_{b_y}}{\sum F_{y_i}} \tag{15}$$

$$\overline{M}_{\theta_i} = M_{\theta_i} \cdot \frac{\Delta V_{b_y}}{\sum F_{y_i}} \tag{16}$$

In these equations, ΔV_{by} represents the incremental base shear force in the seismic excitation lateral direction, ΣF_{yi} is the sum of the lateral forces and $(F_{v})M_{\rm fi}$ is defined previously.

The proposed pushover technique, incorporating lateral loads (\bar{F}_{yi}) and torsional moments $\bar{M}_{\theta i}$ can be easily implemented in a practical structural analysis platform [18].

Computation of the components of seismic modification factors

The seismic modification factor, denoted as R in codes [4, 5] and referred to as q in Eurocode 8 [3], is commonly used in highway bridge seismic design regulations to estimate the design force of a structure analysed using linear methods while exhibiting a nonlinear response. Furthermore, the R-factor directly depends on the components influencing the energy dissipation capacity of the structure, such as the ductility, added viscous damping, and strength reserves resulting from the redundancy and overstrength of individual members.

The pushover curve was idealised using a bilinear response curve (Figure 4).

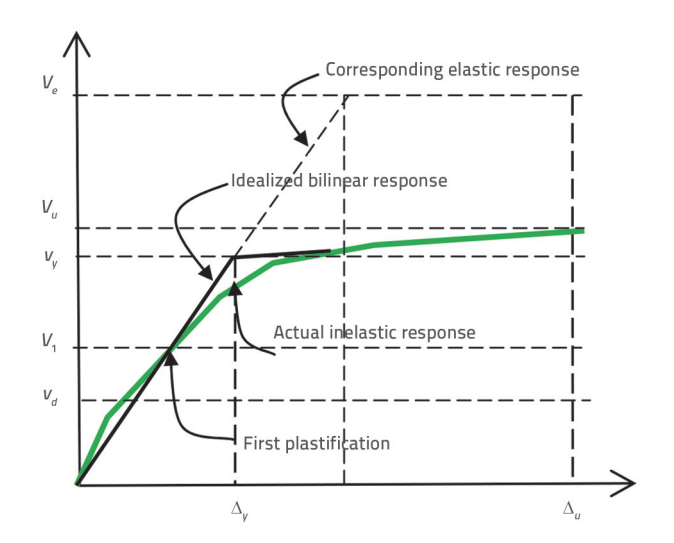


Figure 4. Schematic representation of the relationship between base shear and mid-span displacement of the bridge

The R-factor can be expressed as follows:

$$R = \frac{V_e}{V_d} \tag{17}$$

where V_{e} and V_{d} represent the maximum elastic and design forces, respectivel

5.1. Over-strength factor

Structures often possess a significant reserve strength, which reflects the extent to which the actual strength exceeds the design strength, accounting for material properties and structural redundancy. Based on references [29, 30], the overstrength factor, denoted as Ω), is expressed as the ratio of the ultimate base shear (V_u) at bridge supports (piers and abutments) to the design strength (V_d) .

In this study, V_d is determined based on the elastic design spectrum [5].

$$\Omega = \frac{V_u}{V_d} \tag{18}$$

where V_u represents the ultimate base shear capacity, which represents the maximum lateral force that the structure can resist before failure. Using the elastic design spectrum, the design base shear (. can be estimated as follows:

$$V_d = M \cdot S_{ad} \tag{19}$$

where (M) is the total mass of the bridge and $S_{a,d}$ (T) is the pseudo-acceleration corresponding to the fundamental period of the bridge [5].

5.2. Ductility factor

The ductility factor, denoted as (R_{μ}) , is directly related to the intrinsic properties of the structure, including the fundamental period of vibration (T), damping, ductility, and the characteristics of seismic excitation. Several expressions for (R_{μ}) have been proposed in previous studies [31, 32].

In this study, the expression proposed by [31] is utilised to estimate the kinematic ductility factor (R,) owing to its simplicity.

$$R_{y} = 1$$
 for $T < 0.2$ s (20.a)

$$R_{..} = \sqrt{2\mu - 1}$$
 for 0,2 s < T < 0,5 s (20.b)

$$R_{,,} = \mu$$
 for $T > 0.5$ s (20.c)

where (μ) represents the global ductility ratio, defined as the ratio of the ultimate limit state displacement (δ_u) at the mid-central span of the bridge to the yield displacement (δ_v), expressed as:

$$\mu = \frac{\delta_U}{\delta_V} \tag{21}$$

In most BGBs, the fundamental period (7) exceeds 0.5 seconds. Within this range, Eq. (20) simplifies to

5.3. Seismic modification factor

As shown in Figure 4, the design behaviour factor for a specific structure is given by.

$$R = \frac{V_e}{V_d} = \frac{V_e}{V_u} \cdot \frac{V_u}{V_d} = R_{\mu} \cdot \Omega \tag{22}$$

Following the simplified procedure proposed by [24], the R-factor is estimated as the product of the ductility factor (R_p), the overstrength factor, and the redundancy factor (R_p) [33].

$$R = R_{_{II}} \cdot \Omega \cdot R_{_{R}} \tag{23}$$

According to the table in [3], the redundancy factor (R_R) is assumed to be equal to unity.

Thus, the R-factor simplifies to:

$$R = R_{\mu} \cdot \Omega \tag{24}$$

6. Failure criteria

The numerical results of the seismic behaviour factors were examined using two collapse limit states, and the overall collapse of the bridge structure occurred when one of these two failure limit states was exceeded.

- Plastic Hinge Formation: The collapse damage-state criterion is associated with the formation of plastic hinges at critical locations on a bridge. The development of these hinges was tracked in the pushover analysis, and thresholds were defined to indicate when the structure reached a failure state. This criterion was established by limiting the rotational ductility demands at the ends of the bridge piers, ensuring that they remain within the permissible rotational ductility limits (θ/θ_u) = 1, that is when the ratio
- According to the RPOA [5] and EC8 [3] seismic design codes, the drift ratio limit was set to 2.5 %.

The proposed pushover curve and the progression of the plastic-hinge development at bridge piers are presented in Figure 5.

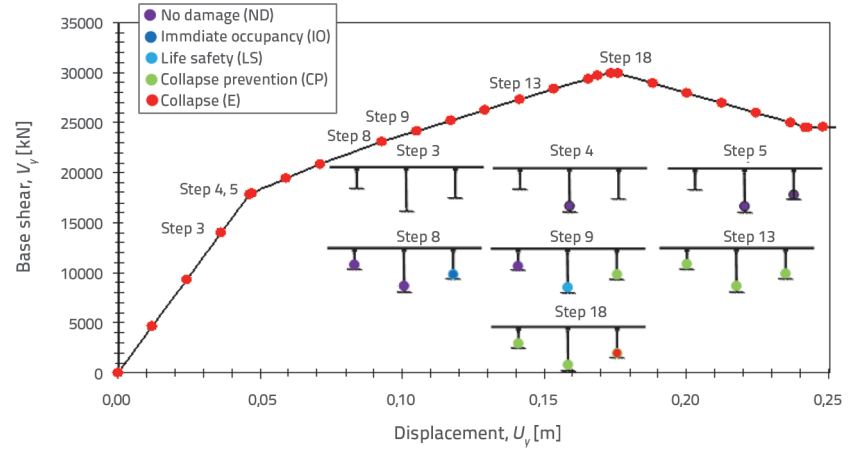


Figure 5. Proposed pushover curve and progression of plastic hinge development at the reference BGB piers

In accordance with seismic design codes [11, 22], the performance levels and corresponding damage states are defined as follows.

Performance level	Damage description
No Damage (ND)	Almost no damage
Immediate Occupancy (IO)	Very slight damage
Life Safety (LS)	Moderate damage
Collapse Prevention (CP)	Severe damage
Collapse (E)	Total failure

7. Selection of earthquake ground motion records

For this study, an ensemble of eight historical earthquake records with varying characteristics, ranging from 0.22g to 0.60g (where g denotes the acceleration due to gravity), was selected from the PEER database (https://peer.berkeley.edu/peer-strong-ground-motion-databases). These records were used to estimate the components of the R-factors of the reference BGB through IDA. Each selected ground motion was scaled to a PGA between 0.1g and 2g, thereby covering the entire structural response spectrum from initial yielding to ultimate collapse.

This study followed the following guidelines recommended in the Eurocode 8 provisions for the selection of recorded timehistories [3]:

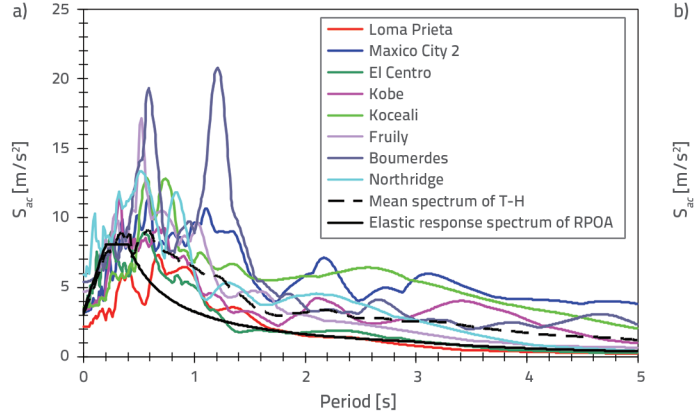
- An appropriate number of records should be used (typically three to seven).
- The mean zero-period spectral response acceleration values should not be less than ,where is the soil factor and is the design ground acceleration)
- Within the period range where is the fundamental period of the structure in the direction of the applied accelerogram, the mean 5 % damping elastic spectrum, calculated from all time-histories, should not be lower than 90 % of the corresponding 5 % damping elastic design spectrum.

Table 1 presents the main characteristics of the historical earthquakes considered in this study.

For illustration, figure 6 presents the elastic response spectra corresponding to the selected historical earthquakes for 5 % damping, together with the mean spectrum of the time-history (T-H) analysis scaled to the reference PGA. The design spectrum reported by [26] is also shown in the figure. The site of the case study, a box girder bridge, is characterised by firm ground conditions (dense soil and gravel), corresponding to a soil factor of S = 1.1 and characteristic periods $T_1 = 0.15$ s and $T_2 = 0.40$ s. The bridge is assumed to be located in a high-seismicity zone with a PGA of 0.33 g.

Table 1. Historical earthquakes considered in this study

ID earthquake	Earthquake name and country	Station name	Magnitude (Mw)	PGA [g]
1	Loma Prieta, USA, 1989	Golden Gate Bridge	6.93	0.22
2	Mexico, 1985	Mexico City	8.10	0.33
3	Imperial Valley, USA, 1940	El Centro, CA – Array Sta 9	6.70	0.35
4	Kobe, Japan, 1995	Kakogawa	6.90	0.34
5	Kocaeli, Turkey, 1999	Düzce	7.51	0.36
6	Friuli, Italy, 1976	Southern Alps	6.50	0.48
7	Boumerdès, Algeria, 2003	Dar El Beida	6.80	0.50
8	Northridge, USA, 1994	Sylmar County Hospital	6.80	0.60



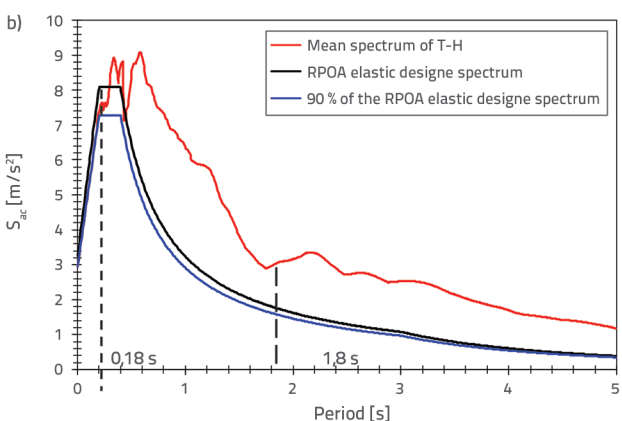


Figure 6. a) Elastic response spectra of the selected historical earthquakes for 5 % damping and the mean spectrum of the Time-History (T-H) analysis scaled to the reference PGA; elastic response spectrum of RPOA (2008); b) Mean values of all spectra

Modal	odal Period [s] Modal participating mass factors (U)		ng mass factors (U)	Modal participation factors $(\Gamma_{_{_{\! \! \! \! \! \! \! \! \! \! \! \! \! \! \! \! \! $	
orders	Period [S]	Lateral direction (U _y)	About longitudinal axis (R _x)	Lateral direction ($\Gamma_{_{y}}$)	About longitudinal axis ($\Gamma_{\rm Rx}$)
1	0.904	0.540	<u>0.026</u>	-2.356	-6.977
2	0.463	0.011	0.000	0.329	-0.202
3	0.302	0.152	0.004	1.249	-2.576
4	0.218	0.001	0.032	-0.083	7.683
5	0.216	0.000	0.000	-0.020	0.509
6	0.202	0.000	0.000	0.011	0.280
7	0.183	<u>0.135</u>	0.079	-1.177	-12.066
8	0.168	0.005	0.004	0.220	2.874
9	0.166	0.008	0.012	-0.287	4.716
10	0.125	0.000	0.000	-0.022	-0.019
11	0.120	0.005	0.167	0.218	17.511

Table 2. Dynamic properties of the reference BGB

8. Results and discussions of the first part

8.1. Modal analysis of the reference BGB

Load-dependent Ritz orthogonal vectors (LDR) [28, 34] were employed because of their advantage in performing static nonlinear analyses under force distribution models applied in the lateral direction of the reference BGB.

Table 2 presents the first 11 natural vibration periods along with the associated modal participating mass factors and modal participation factors in the lateral (Y-axis) and longitudinal (X-axis) directions.

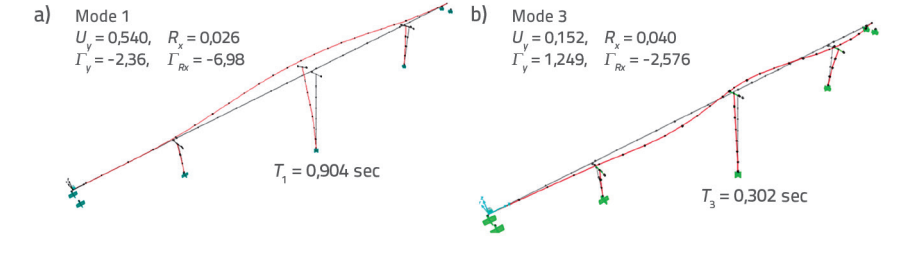
As shown in Table 2 and the mode shapes illustrated in Figure 7, the dominant vibration mode occurred in the lateral direction (i.e. the most flexible) with a first-mode period of 0.904 s. The seventh lateral mode was highly coupled with the torsional mode (= 0.135, = 0.079) owing to the irregularity of the studied

bridge. However, the eleventh vibration mode primarily consisted of torsion (= 0.005, = 0.167) about the longitudinal axis of the bridge. Table 2 also shows that the lateral translational modal participating mass ratio for the dominant mode was only 54 %. Consequently, the higher modes significantly contributed to the seismic response in the lateral direction (approximately 46 %). Therefore, the first elastic mode was insufficient for conducting a lateral nonlinear static pushover analysis on the studied bridge. A pushover analysis based only on the fundamental mode fails to adequately capture the seismic effects owing to the considerable influence of higher modes.

In conclusion, the fundamental mode contributes to the lateral response but does not fully dominate the seismic behaviour of the bridge. Higher modes (particularly modes 3, 7, and 11) played a crucial role because of their significant modal participation. A more advanced approach such as a multimodal pushover or nonlinear dynamic analysis is required for an accurate seismic

assessment.

A graphical representation of the mode shapes of the bridge showed that the first mode was predominantly translational in the Y-Y lateral direction (indicating greater flexibility in this direction). The seventh vibration mode is dominant in the Y-Y lateral direction and is coupled with the torsional mode of vibration, whereas the eleventh mode is predominantly torsional and weakly coupled with the translational lateral mode.



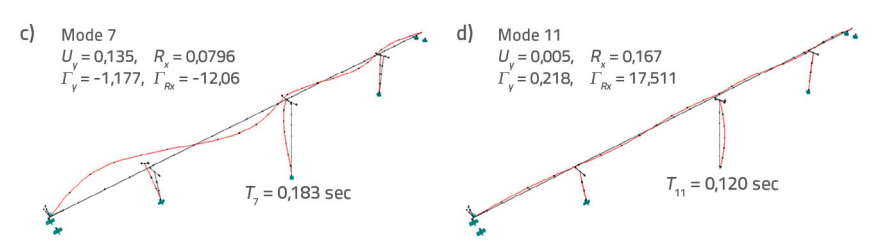


Figure 7. Mode shapes of the bridge and associated dynamic parameters: a) First lateral mode; b) Third lateral mode; c) Lateral mode coupled with torsion; d) Pure torsional mode.

8.2. Development of nonlinear static pushover curves

For comparison purposes, the global pushover curves for the reference BGB in the lateral direction (i.e. the more flexible direction) obtained from the ((CPA)

under the elastic first mode, uniform and upper-bound lateral load patterns, and the proposed pushover technique, including torsional vibration modes, are plotted in Figure 8. In this study, the P-delta effects and gravity loads were considered during nonlinear static pushover analyses. It should also be noted that the possible failures of the abutment backfill system and HDRB devices were not considered.

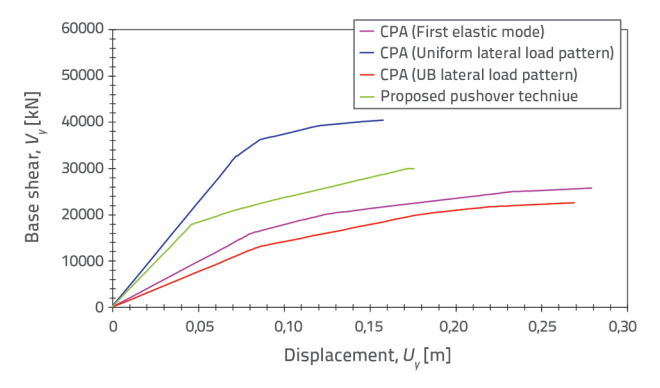


Figure 8. Comparison of global pushover curves for the reference BGB in lateral direction obtained from conventional pushover analysis and the proposed pushover technique

From the capacity curves depicted in Figure 8, it is evident that for the reference BGB, the conventional pushover analysis (CPA) with a uniform lateral load pattern resulted in the highest base shear capacity in the lateral direction compared with the CPA conducted with other lateral load patterns. However, when the midspan of the bridge was pushed well into the inelastic range under the first elastic mode and upper-bound (UB) lateral load patterns, the corresponding base shear was the lowest, while the estimated ductility was higher. In contrast, the proposed pushover technique, which incorporates torsional effects, provides intermediate results, achieving a balance between the strength and deformation capacity compared to the uniform, first elastic, and upper-bound lateral load patterns.

In conclusion, the comparison of the pushover curves demonstrates that the conventional pushover analysis of (First Mode and UB lateral load patterns) underestimates the base shear capacity while providing higher ductility estimations. The Proposed Pushover Technique, which incorporates torsional effects, offers a more accurate representation of the nonlinear response of the studied BGB in accordance with the Eurocode 8 provisions (sections such as Clauses 4.3.3.4.2 (consideration of higher modes) and 4.2.2 (torsional effects)). These clauses

highlight the importance of accounting for higher mode effects and the contribution of torsional effects resulting from mass eccentricity and other structural asymmetries, which are crucial for the seismic assessment of complex geometries such as BGBs.

In addition, Table 3 summarises the ultimate shear strength and the components of the response modification factor (R-factor), including the overstrength factor () and the kinematic ductility (), for the reference box girder bridge (BGB).

As previously noted, the shear capacity at the bridge supports is highest with a uniform load distribution, which also corresponds to a higher overstrength factor (Ω). Furthermore, it should be noted that the ductility factors remain relatively low and exhibit minimal variation between the uniform load model and the proposed pushover technique in this analysis. According to the R-factor values presented in Table 2, the R-factor obtained using the proposed pushover technique is lower than that derived from conventional pushover analysis (CPA). This difference is primarily owing to the significant contribution of the torsional vibration modes to the overall capacity of the reference BGB when using the proposed method.

In conclusion, the proposed pushover technique offers the most realistic and comprehensive approach because it considers torsional effects. It is recommended over conventional CPA methods for more accurate nonlinear seismic assessment of BGBs.

In the next section, the performance and accuracy of conventional pushover analysis and the proposed pushover techniques for the studied BGB are evaluated to determine which approach provides a more accurate prediction of structural behaviour in comparison with the IDA.

8.3. Development of Incremental dynamic pushover curves

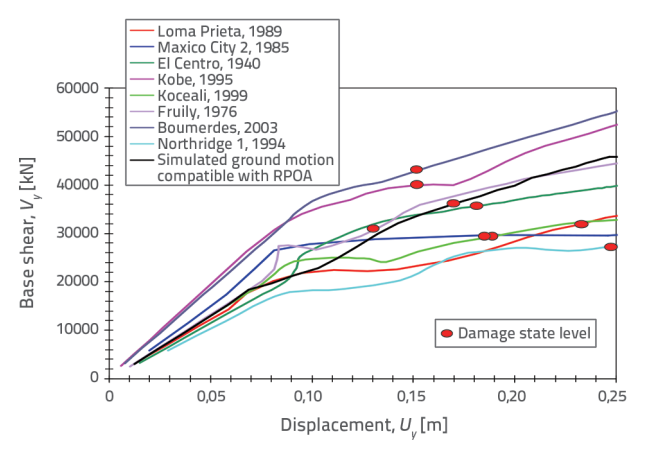
The IDA is one of the most effective approaches proposed in various studies for assessing the seismic capacity of structures [9, 35, 36]. However, generating a capacity curve using IDA is computationally demanding, time-consuming, and cost-effective. This approach involves subjecting a structure to multiple real or simulated seismic ground motions, scaled at different intensity levels. A multirecord incremental dynamic pushover curve was obtained by plotting the maximum shear forces at the bridge supports against the maximum displacement at the control point of the bridge.

Table 3. Ultimate shear strength and R-factor components for the studied BGB

Nonlinear static pushover techniques	V _u [kN]	Ω	\mathbf{R}_{μ}	R
CPA (First elastic mode)	25823	2.49	3.05	7.59
CPA (UB lateral load pattern)	22561	2.17	2.76	5.99
CPA (Uniform lateral load pattern)	40500	3.90	1.97	7.68
Proposed pushover technique	29693	2.86	1.92	5.49

In the first step, the IDA capacity curves in the lateral direction of the box girder bridge, subjected to a suite of eight past historic earthquakes with different ground motion characteristics ranging from 0.22 g to 0.60 g, are developed. The Newmark average acceleration method was used for the nonlinear time history analysis. Rayleigh damping was considered, and the mass- and stiffness-proportional coefficients were evaluated for 5 % damping, which occurred in the first two vibration modes of the bridge's analytical model.

Figure 9 shows the developed IDA curves, illustrating the relationship between the base shear at the bridge supports and the maximum displacement at the control point in the critical lateral direction (Y-axis) of the studied BGB subjected to eight historical earthquake records, as well as a simulated ground motion compatible with the design spectrum RPOA [5].



Slika 9. Krivulje sposobnosti nosivosti iz inkrementalne dinamičke Figure 9. IDA capacity curves of the studied BGB subjected to eight historical earthquake records

In the Figure, the red points represent the collapse damage state level observed for the bridge under each record of past historic earthquakes and the simulated ground motion compatible with the RPOA design spectrum [5]. These points correspond to the ultimate displacement values at the control point and base shear at the bridge supports. They are crucial for determining

seismic parameters such as the ultimate shear strength, the overstrength factor (), the kinematic ductility factor (), and the R-factor. These parameters play a significant role in assessing the ductile response of a structure and have critical implications for the brittle failure modes. The results obtained from the IDA are listed in Table 4.

8.4. Comparison of global pushover and incremental dynamic curves

In this subsection, the results of the global pushover curves for the reference BGB in the lateral direction obtained from the conventional pushover analysis and the proposed pushover technique are compared with those of the mean dynamic pushover curves obtained from IDA. Also, the mean values of IDA, along with plus and minus one standard deviation are depicted in Figure 10.

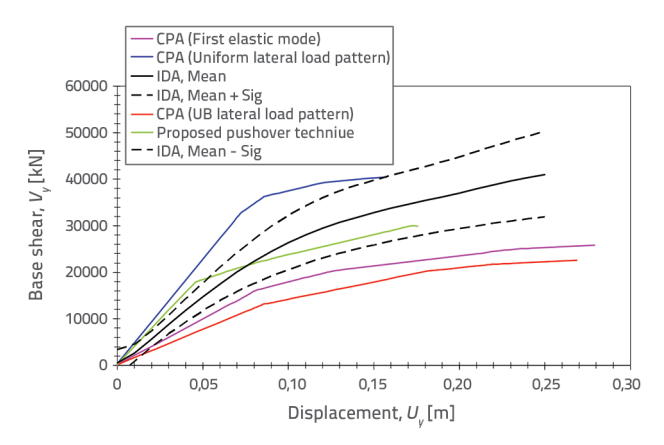


Figure 10. Comparison of Pushover and incremental dynamic analysis (IDA) Curves

From Figure 10, it should be noted that the capacity curves for the studied BGB are underestimated by the first elastic mode and upper-bound lateral load patterns, and overestimated by the uniform lateral load pattern. This is because their pushover curves produce results outside the range of (mean $-\sigma$) and

Table 4. Ultimate shear strength and R-factor	r components for the studied BGB
---	----------------------------------

Ground motion	V _u [kN]	Ω	\mathbf{R}_{μ}	R
Loma Prieta, USA, 1989	30702	2.96	1.78	5.27
Mexico, 1985	29509	2.84	2.15	6.11
Imperial Valley, USA, 1940	35215	3.39	1.81	6.14
Kobe, Japan, 1995	40057	3.86	1.34	5.17
Kocaeli, Turkey, 1999	30837	2.97	1.62	4.81
Friuli, Italy, 1976	30993	2.99	1.20	3.59
Boumerdès, Algeria, 2003	47602	4.40	1.35	5.94
Northridge, USA, 1994	27580	2.66	1.75	4.66
Simulated ground motion compatible with RPOA	37703	3.63	1.62	5.88
Mean value	34466	3.30	1.62	5.36

Nonlinear static pushover techniques	CPU time [s]	Ω	R_{μ}	R	
CPA (First elastic mode)	31	2.49 (-25 %)	3.05 (+88 %)	7.59 (+42 %)	
CPA (UB lateral load pattern)	80	2.17 (-34 %)	2.76 (+70 %)	5.99 (+12 %)	
CPA (Uniform lateral load pattern)	79	3.90 (+18 %)	1.97 (+22 %)	7.68 (+43 %)	
Proposed pushover technique	104	2.86 (-13 %)	1.92 (+19 %)	5.49 (+2 %)	
IDA (Reference value)	6174	3.30	1.62	5.36	
(%): Relative percentage errors compared to the IDA results					

Table 5. Comparison of CPU time, R-factors components and percentage error

(mean $+ \sigma$) values derived from IDA. In contrast, the proposed pushover curve, obtained using the proposed model including torsional vibration modes, falls within the range between (mean $- \sigma$) and (mean $+ \sigma$) of the IDA curve, making it a more realistic representation of the bridge's seismic behaviour.

It can be concluded that the proposed pushover technique, including torsional vibration modes, closely aligns with the IDA mean curve and is a more reliable and realistic method for the nonlinear seismic assessment of BGBs than conventional pushover methods.

In this study, the components of the R-factor presented in Table 3 evaluated in accordance with the methodologies mentioned in Section 4 were compared with the mean values obtained through the inelastic incremental dynamic analysis technique. This step aims to assess the performance and accuracy of the proposed pushover technique, which includes the torsional motion.

The results of the R-factor components, determined through both the conventional (CPA) and proposed pushover techniques, as well as the IDA, are presented in Table 5. The CPU time required to compute the R-factor components is listed in the same table.

From Table 5, it can be observed that for the conventional pushover technique (CPA) with all lateral load patterns except the uniform load pattern, the overstrength parameters obtained were generally lower than those derived from IDA which is considered the reference value. Furthermore, compared with the IDA results, the global ductility values estimated using CPA were significantly higher for the first elastic mode (+88 %) and upper-bound model (+70 %). These differences were primarily due to the neglect of higher-mode contributions in the evaluation of the seismic responses when the two lateral load models were used in the CPA technique.

Furthermore, the global ductility demands estimated from the CPA with a uniform lateral load pattern and the proposed pushover technique were relatively similar, with differences of 22 % for the uniform pattern and 19 % for the proposed model. Notably, the proposed pushover technique considers the torsional vibration modes of the studied bridge, enhancing the accuracy of the seismic behaviour factor evaluation. As indicated in Table 5,the proposed pushover technique yielded an R value of 5.49, which was the closest to the IDA (5.36, 2 % difference), confirming its accuracy in estimating the overall

seismic behaviour. In addition, The CPA and proposed pushover techniques were significantly faster than IDA, with computation times reduced by 99 % (ranging from 31s to 104s compared with 6174s for IDA).

In conclusion, the proposed pushover technique showed good agreement with the IDA results for the R-factor, with a slight increase of approximately 2 %.

It is important to highlight that the CPU time required to estimate the R-factor using the IDA technique (6174 s) was approximately 60 times greater than that required for the proposed pushover technique (104 s). This significant difference in processing time was observed while using a laptop with the following specifications: Intel® Core™ i3-5005U CPU running at 2.00 GHz. This comparison emphasises the computational efficiency of the proposed pushover method, which provides a considerably faster alternative for estimating the R-factor, and proves to be more computationally effective than the IDA technique.

9. Results and discussions of the second part

9.1. Variants of the referenced BGB

In this study, a selection of eighteen continuous prestressed box girder bridges (BGBs) with both identical and varying pier heights is investigated to estimate the seismic modification factors (R) for this category of bridges. These bridges are derived as variants of the reference bridge, and each variant (V) is labelled using the notation V_i - κ , where *i* refers to the number of spans (03, 04, 05), *j* indicates the number of piers (02, 03, 04), and the character κ represents the pier height classification: short (S), medium (M), or tall (T). The heights of the short, medium, and tall piers were 15.95 m, 26.65 m, and 50.35 m, respectively. For example, the reference bridge shown in Figure 1 is labelled V43-STM, which refers to a bridge with four spans, three piers, and Short, Tall and Medium piers in that specific order. The key parameters used for the classification were the number of spans, number of piers, and height of the piers. The variants were classified based on modifications to these parameters, allowing for a comprehensive investigation of the influence of geometric changes on the seismic behaviour. The basic characteristics of the different variants of the reference BGB (V43-STM) analyzed in this study are listed in Table 6.

Table 6.Characteristic of variants of the referenceBGB (V43-STM)

Variants of V43-STM	No. of spans	Span length [m]	No. of piers	Pier heights [m]	Total length [m]	
Variants of the referencV43-STM with equal pier heights						
V32-S	3	42.6 + 81.8 + 42.6	2	15.95	167	
V32-M	3	42.6 + 81.8 + 42.6	2	26.65	167	
V32-T	3	42.6 + 81.8 + 42.6	2	50.35	167	
V43-S	4	42.6 + 2 × 81.8 + 42.6	3	15.95	248.8	
V43-M	4	42.6 + 2 × 81.8 + 42.6	3	26.65	248.8	
V43-T	4	42.6 + 2 × 81.8 + 42.6	3	50.35	248.8	
V54-S	5	42.6 + 3 × 81.8 + 42.6	4	15.95	330.6	
V54-M	5	42.6 + 3 × 81.8 + 42.6	4	26.65	330.6	
V54-T	5	42.6 + 3 × 81.8 + 42.6	4	50.35	330.6	
	Varia	ants of the reference V43-S	TM with unequa	pier heights		
V32-TS	3	42.6 + 81.8 + 42.6	2	50.35; 15.95	167	
V32-SM	3	42.6 + 81.8 + 42.6	2	15.95; 26.65	167	
V32-TM	3	42.6 + 81.8 + 42.6	2	50.35; 26.65	167	
V43-STM	4	42.6 + 2 × 81.8 + 42.6	3	15.95; 50.35; 26.65	248.8	
V43-MST	4	42.6 + 2 × 81.8 + 42.6	3	26.65; 15.95; 50.35	248.8	
V43-TMS	4	42.6 + 2 × 81.8 + 42.6	3	50.35; 26.65; 15.95	248.8	
V54-MTTS	5	42.6 + 3 × 81.8 + 42.6	4	26.65; 50.35; 50.35; 15.95	330.6	
V54-STTS	5	42.6 + 3 × 81.8 + 42.6	4	15.95; 50.35; 50.35; 15.95	330.6	
V54-MTTM	5	42.6 + 3 × 81.8 + 42.6	4	26.65; 50.35; 50.35; 26.65	330.6	

9.2. Evaluation of R-factors for different variants of real BGBs

The R-factor components for each variant of the reference BGB were determined at the ultimate limit state using the proposed pushover technique described in Subsection 4.2, which is more computationally efficient than the conventional IDA.

9.2.1. Comparaison of R-factor components for variants of the reference V43-STM with equal pier heights

The components of R-factors including the over strength factors (Ω) as well as the associated ductility factors (Rµ) for different variants of the referenced BGB (V43-STM) are presented in

Tables 7. The R-factor is determined as the product of two components Ω and $R\mu$, such that $R = \Omega \cdot R\mu$.

From Table 7, it can be observed that the V32-S variant with equal pier heights exhibits the greatest overstrength ($\Omega=3.80$), indicating the highest reserve capacity beyond the design base shear. In contrast, the V54-M and V54-T variants exhibit the smallest overstrength values, equal to 1.98 and 1.99, respectively, indicating that these structures operate closer to their design limits with minimal reserve capacity, increasing vulnerability under extreme seismic loads.In contrast, It is also observed that the V32-S variant exhibits the lowest ductility factor ($R\mu=1.10$), while the V54-T variant shows the highest values $R\mu=2.67$ and R=5.31, indicating a greater capacity of the latter to dissipate seismic

Table 7. Components of R-factors for the variants of the referenced BGB (V43-STM) with equal pier heights

Variants of V43-STM	Overstrength (Ω)	Ductility (R _µ)	R-factor (R)
V32-S	<u>3.80</u>	<u>1.10</u>	4.18
V32-M	2.51	1.47	3.69
V32-T	2.69	1.58	4.25
V43-S	2.83	<u>1.65</u>	4.67
V43-M	2.02	2.31	4.67
V43-T	2.01	2.09	4.20
V54-S	3.23	<u>1.31</u>	4.23
V54-M	1.98	2.31	4.57
V54-T	1.99	2.67	5.31

energy through inelastic deformation and better seismic performance (higher R-values).

In general, the rigid variants with equal pier heights, especially those with shorter piers (e.g., V32–S, V43–S, and V54–S), tend to exhibit higher overstrength (Ω) due to their increased stiffness. This suggests a significant safety margin, implying that these structures can resist seismic forces substantially greater than those accounted for in the seismic design, whereas flexible variants of equal height (e.g. V54–T) generally provide greater ductility and better seismic performance (higher R-values) but show lower overstrength owing to their increased flexibility and deformation capacity.

9.2.2. Comparaison of R-factor components for variants of the reference V43-STM with unequal pier heights

Table 8 presents the components of the R-factors for the different variants of the reference BGB (V43-STM) with unequal pier heights.

From Table 8, it can be observed that the referenced BGB(V43-STM) exhibits moderate overstrength and the highest ductility (, which leads to better seismic performance with an R-factor

of 5.49. It is also noted that the V32-TM variant shows the lowest overstrength (Ω = 2.69) and R-factor(R = 3.79) values, indicating reduced seismic capacity.

A comparison between variants with equal (e.g. V54-T) and unequal (e.g. V54-MTTM) pier heights revealed that, in general, variants with unequal pier heights exhibited increased overstrength demands and reduced global ductility. This emphasises the necessity for customised R-factor assessments to account for geometric irregularities and their impact on the seismic performance.

In conclusion, selecting appropriate pier height configurations and optimising the overstrength and ductility factors are essential for enhancing the seismic resilience of box-girder bridges. Variations in pier height can significantly influence the structural response during seismic events, affecting both the distribution of seismic forces and the deformation capacity. The precise evaluation of these parameters allows for improved design strategies that mitigate the adverse effects of geometric irregularities and ensure better energy dissipation and structural stability under seismic loads.

The chart compares the R-factors for various BGB configurations. Blue bars represent variants with equal pier heights, whereas orange bars indicate variants with unequal pier heights. The x-axis denotes the variant configurations and the y-axis shows the corresponding R-factor values.

As illustrated in Figure 11, the bar chart indicates that variant configurations with unequal pier heights generally exhibit higher R-factors than those with equal pier heights (e.g. the referenced BGB, V43-STM). However, in certain cases, configurations with equal pier heights exhibited better R-factors (e.g. V54-T) or yielded comparable results in specific models (e.g. V43-T).

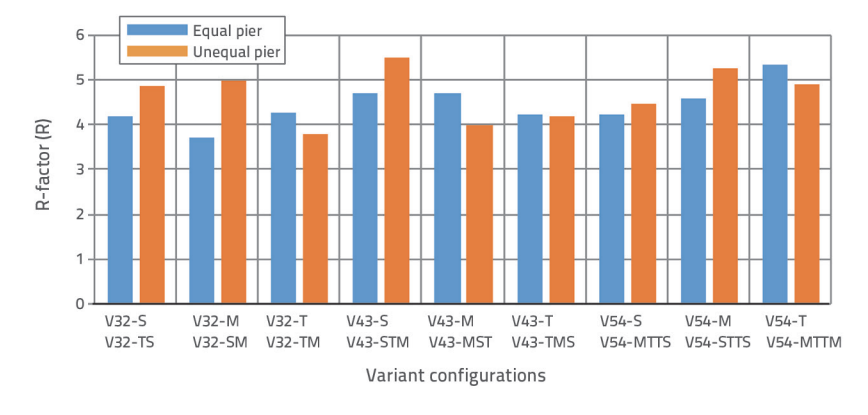


Figure 11. Comparison of R-Factors BGB variants with equal and unequal pier heights

Table 8. Components of R-factors for the variants of the referenced BGB (V43-STM) with unequal pier heights

Variants of V43-STM	Overstrength (Ω)	Ductility (R _µ)	R-factor (R)
V32-TS	3.46	1.40	4.84
V32-SM	3.18	1.56	4.96
V32-TM	2.69	1.41	3.79
V43-STM	2.86	1.92	5.49
V43-MST	3.09	1.29	3.99
V43-TMS	2.87	1.45	4.16
V54-MTTS	3.05	1.46	4.45
V54-STTS	3.33	1.57	5.23
V54-MTTM	2.80	1.75	4.90

9.3. Prediction of R-factor of BGBs and comparison with the Algerian highway bridge design seismic regulation

For box girder bridges (BGBs) in the transverse direction, the calculated R-factor values range from 3.69 to 5.49, with an average value of 4.53 and a standard deviation of 0.52. These results indicate higher energy dissipation and structural ductility compared with the values prescribed by the Algerian highway bridge design seismic regulation RPOA [5], which specifies an R-factor range between 1.5 and 3.5. This discrepancy suggests that RPOA provisions may underestimate the actual inelastic deformation capacity of box girder bridges, potentially leading to conservative seismic design provisions.

The values of the R-factor estimated by the RPOA [5] have been established for all categories of bridges built in Algeria since 2008, the year in which the public works sector adopted the first Seismic Regulation for Civil Engineering Structures (RPOA-2008), the first of its kind since independence.

However, based on the results of this study, it is recommended to select bridges capable of developing large plastic deformations while maintaining structural stability in areas of high seismicity. This corresponds to structures within the high-ductility class (DCH), such as box girder bridges, which generally exhibit behaviour factor values greater than 3.5, depending on the adopted structural system. Increasing the energy dissipation capacity enhances resistance to extreme seismic demands.

Based on this study, it is recommended that the Ministry of Public Works, during the next revision of the regulation, advocate for behavior factors ranging between 3.5 and 5.5 for structures within the DCH, particularly for box girder bridges.

10. Conclusion

The first part of this study presents a numerical investigation of the components of the R-factor, including the overstrength factor and global ductility, for the reference BGB using Conventional Pushover Analysis and the proposed pushover techniques. The results are compared with those obtained from the inelastic IDA method, based on a suite of eight historical earthquakes with ground motion characteristics ranging from 0.22g to 0.60g, as well as a simulated ground motion compatible with the design spectrum of the RPOA. In the second part, eighteen continuous prestressed BGBs with both equal and unequal pier heights, representing regular and irregular configurations, are analysed to estimate the R-factor in the transverse direction using the proposed pushover technique. The resulting R-factor values are then compared with the provisions of the RPOA. Based on the results of this investigation, the following key conclusions can be drawn.

Regarding the first part of this study:

- For the reference BGB, the first mode exhibits the highest modal participating mass factor (in the lateral direction, but does not fully govern the bridge's seismic behaviour. The distribution of modal participating mass factors in higher modes indicates that these, particularly those associated with rotational effects about the longitudinal axis, also play a crucial role in the seismic response of the studied BGB.
- The CPA using the first elastic mode distribution is not appropriate for the studied bridge when performing nonlinear static pushover analysis. A more advanced approach, such as multimodal pushover including torsional vibration modes or IDA, is required for an accurate seismic assessment.
- The CPA technique, based on the first mode and upper-bound lateral load patterns, underestimates the base shear capacity while overestimating ductility. In contrast, the proposed pushover technique, which accounts for torsional vibration modes, provides a more accurate estimation of the bridge's nonlinear response, particularly for irregular and complex geometries such as BGBs, in accordance with Eurocode 8 provisions. This emphasises the need to consider higher modes and torsional behaviour in seismic performance assessments of BGBs.
- The proposed pushover curve, which closely corresponds to the IDA mean curve, offers a more realistic and comprehensive approach. It is preferable to conventional CPA methods (elastic first mode, uniform, and upperbound load distribution models) for accurate nonlinear seismic assessment of BGBs.
- For practically the same level of accuracy, the proposed pushover technique requires significantly less computational effort to estimate the R factor of the studied BGB compared with the IDA procedure, with only a slight increase of approximately 2 %.

Regrading the second part of this study:

- In general, rigid variants of equal height, particularly those with shorter piers (e.g., V32-S, V43-S, and V54-S), exhibit higher overstrength (Ω) owing to their increased stiffness. This indicates a considerable safety margin, suggesting that such structures can withstand seismic forces substantially greater than those accounted for in design.
- Compared with rigid variants, flexible variants of equal height (e.g., V54-T) provide greater ductility and improved seismic performance (higher R-values) but display lower overstrength due to their higher flexibility and deformation capacity.
- In regions of severe seismicity, flexible box girder bridges are
 often preferred for their greater ductility and higher R-factors.
 By contrast, rigid box girder bridges are more suitable where
 enhanced overstrength and stiffness are required, offering
 safety margins against moderate ground motions.

- The number of spans, pier heights, and their configuration strongly influence the seismic behaviour of BGBs. Bridges with unequal pier heights introduce geometric irregularities, which may amplify seismic demands and reduce overall resistance. This variability underscores the need for careful planning and tailored designs to ensure reliable performance during earthquakes.
- Based on the results of this study, it is recommended that the Ministry of Public Works, in the next revision of the regulations, advocate behaviour factors ranging from 3.5 to 5.5 for bridge structures classified under the DCH, particularly for box girder bridges. This adjustment would provide a more accurate representation of the seismic performance of such structures.

REFERENCES

- [1] Ouanani, M., Tiliouine, B.: Effects of foundation soil stiffness on the 3-D modal characteristics and seismic response of a highway bridge, KSCE J Civ Eng., 19 (2015), pp. 1009-1023, https://doi.org/10.1007/s12205-013-0435-5
- [2] Kehila, F., Khelfi, M., Belkacem, M.A.: Scalar and vector-valued fragility analysis of typical Algerian RC bridge piers, Gradevinar, 75 (2023) 6, pp. 577-590, https://doi.org/10.14256/JCE.3630.2022
- [3] European Committee for Standardization (CEN): Eurocode 8. design for earthquake resistance Part 1: General rules: seismic actions and rules for buildings: European Standard EN 1998-1, Brussels: CEN; 2004.
- [4] International Conference of Building Officials: Uniform building code. Whittier, CA, USA: International Conference of Building Officials, 1994.
- [5] RPOA Part 1: Ponts, Règles parasismiques applicables au domaine des ouvrages d>arts, Algeria; 2008.
- [6] Isakovic, T., Fischinger, M.: Higher modes in simplified inelastic seismic analysis of single column bent viaducts, Earthq Eng Struct Dyn,. 35 (2006) 1, pp. 95-114, https://doi.org/10.1002/eqe.535
- [7] Paraskeva, T.S., Kappos, A.J., Sextos, A.G.: Extension of modal pushover to seismic assessment of bridges, Earthq Eng Struct Dyn,. 35 (2006) 11, pp. 1269-1293, https://doi.org/10.1002/eqe.582
- [8] Di Re, P., Bernardin, D., Ruta, D., Paolone, D.: Pushover analyses of slender cantilever bridge piers with strength and ductility degradation, KSCE J Civ Eng., 28 (2024), pp. 836–848, https://doi. org/10.1007/s12205-024-0940-8
- [9] Ganjehei, H., Zarfam, P., Ghafory-Ashtiany, M.: Innovative method for incremental dynamic analysis curves in semi-isolated bridges, Građevinar, 75 (2023) 4, pp. 343-354, https://doi.org/10.14256/ ICE.3065
- [10] Vamvatisikos, D., Cornell, C.A.: Direct estimation of seismic demand and capacity of multi-degree of freedom systems through incremental dynamic analysis of single degree of freedom approximation, J Struct Eng., 131 (2005) 4, pp. 589-599, https://doi.org/10.1061/(ASCE)0733-9445(2005)131:4(589)
- [11] Federal Emergency Management Agency; FEMA 440. Improvement of nonlinear static seismic analysis procedures, Washington, DC, USA: FEMA, 2005.
- [12] Ranjit, S.A., Evgenia, G., Marco, R., Theodoros, T.: Pushover analysis of inelastic seismic behaviour of greveniotikos bridge, J Bridg Eng., 7 (2002) 2, pp. 115-126, https://doi.org/10.1061/ (ASCE)1084-0702(2002)7:2(115)

- [13] Sai, B.E.V., Samba, M.S., Mohan, G.G.: A study on behaviour of bridge piers in various seismic zonal conditions, Int J Eng Trends Technol, 11 (2020) 1, pp. 129-138.
- [14] Muhammad, J.B., Muhammad, W., Muhammad, A.S., Bakht, Z., Mahmood, A., Mohanad, M.S.S.: Response modification factors for multi-span reinforced concrete bridges in Pakistan, Buildings, 12 (2022) 7, Paper 921, https://doi.org/10.3390/buildings1207092
- [15] Michael, C.C., Joseph, K.Q.: Response modification factors for seismically isolated bridges, Tech Rep MCEER, 1998.
- [16] Ehsan, M., Shooshtari, A.: A multimode adaptive pushover procedure for seismic assessment of integral bridges, Adv Civ Eng., (2013), pp. 1-13, https://doi.org/10.1155/2013/941905
- [17] Alessandro, V.B., Camillo, N., Davide, L., Gabriele, F., Bruno, B.: IMPA, incremental modal pushover analysis for bridges, Applied Sci., 10 (2020) 12, Paper 4287, https://doi.org/10.3390/app10124287
- [18] Computers and Structures Incorporation: SAP2000 nonlinear computer software version 2014. Berkeley, California, CSI, 2014.
- [19] California Department of Transportation: Seismic design criteria: design manual, Version 1.6. Sacramento, CA, USA: Caltrans, 2010.
- [20] Priestley, M.J.N., Seible, F., Calvi, G.M.: Seismic design and retrofit of bridges, Wiley, 1995.
- [21] Mander, J.B., Priestley, M.J.N.: Observed stress-strain behavior of confined concrete, J Struct Eng., 114 (1988) 8, pp. 1827-1849, https://doi.org/10.1061/(ASCE)0733-9445(1988)114:8(1827)
- [22] Federal Emergency Management Agency. FEMA 356/ASCE. Seismic rehabilitation prestandard. Washington, DC, USA: FEMA; 2000.
- [23] Ouanani, M., Sandjak, K., Khelafi, A.M.: Performance sismique des systèmes d'isolation dans le comportement dynamique d'un pont caisson type, Algérie Equipement, 2021.
- [24] Applied Technology Council: ATC-40. Seismic evaluation and retrofit of concrete buildings, Redwood City, CA, USA, ATC, 1996.
- [25] Saiidi, M., Sozen, M.A.: Simple non- linear seismic analysis of RC structures, J Struct Div., 107 (1981) 5, pp. 937-951, https://doi. org/10.1061/JSDEAG.0005714
- [26] Krawinkler, H., Seneviratna, G.: Pros and cons of a pushover analysis of seismic performance evaluation, Eng Struct., 20 (1998) 4-6, pp. 452-464, https://doi.org/10.1016/S0141-0296(97)00092-8

- [27] Jan, T.S., Liu, M.W., Kao, Y.C.: An upper-bound pushover analysis procedure for estimating the seismic demands of high-rise buildings, Eng Struct., 26 (2004) 1, pp. 117-128, https://doi.org/10.1016/j.engstruct.2003.09.003
- [28] Chopra, A.K.: Dynamics of structures: theory and applications to earthquake engineering, 6th ed. Pearson, 2023.
- [29] Mitchell, D., Paultre, P.: Ductility and overstrength in seismic design of reinforced concrete structures, Can J Civ Eng., 21 (1994) 6, pp. 1049-1060, https://doi.org/10.1139/194-109
- [30] Kappos, A.J.: Evaluation of behavior factors on the basis of ductility and overstrength studies, Eng Struct., 21 (1999) 9, pp. 823-835, https://doi.org/10.1016/S0141-0296(98)00050-9
- [31] Veletsos, A., Newmark, N.: Effect of inelastic behavior on the response of simple systems to earthquake motions, In: Proceedings, Second World Conference on Earthquake Engineering, (1960), pp. 895-912, Japan.

- [32] Fajfar, P.: A nonlinear analysis method for performance based seismic design, Earthq Spectra, 16 (2000) 3, pp. 573-592, https://doi.org/10.1193/1.1586128
- [33] Itani, A., Gaspersic, P., Saiidi, M.: Response modification factors for seismic design of circular reinforced concrete bridge columns, ACI Struct J., 94 (1997) 1, pp. 23–30.
- [34] Wilson, E.L., Yuan, M.W., Dicken, J.M.: Dynamic analysis by direct superposition of ritz vectors, Earthq Eng Struct Dyn., 10 (1982) 6, pp. 813-821.
- [35] Gerami, M., Mashayekhi, A.H., Siahpolo, N.: Computation of R factor for steel moment frames by using conventional and adaptive pushover methods, Arab J Sci Eng., 42 (2017) 3, pp. 1025-1037, https://doi.org/10.1007/s13369-016-2257-5
- [36] Mwafy, A.M., Elnashai, A.S.: Static pushover versus dynamic collapse analysis of RC buildings, J Eng Struct., 23 (2001) 5, pp. 407-424, https://doi.org/10.1016/S0141-0296(00)00068-7